Journal of Engineering Research and Technological Innovations.
[JERTI] Vol. 1, No 2, 9 - 32 (2026)
https://journals.kwasu.edu.ng/index.php/jerti ISSN: 3093-0863

Process Optimization of Neem (Azadirachta indica) Oil Extraction using a Semi-Automated Screw Expeller for Coating Applications

A. T. Opobiyi [1,*] R. A. Busari[1], A. Zubair[2], A. I. Oyebanji[3],

[1]Department of Food and Agricultural Engineering, Kwara State University, Malete, P.M.B 1530, Kwara State, Nigeria
[2]Department of Agricultural Engineering, Kwara State Ministry of Agriculture and Rural Development, Ilorin, P.M.B. 1383, Kwara State, Nigeria
[3]Postharvest Engineering Research Department, Nigerian Stored Products Research Institute, Km 3, Asa Dam Road, P.M.B. 1489, Ilorin, Kwara State, Nigeria

[1]toshoopobiyi@yahoo.com,[1]rasheed.busari@kwasu.edu.ng,[2]ndagimaliki@gmail.com,[3]obanjiometer87@gmail.com
*Corresponding Author: toshoopobiyi@yahoo.com ; Tel.: +234-(0)-703-1314-321

ABSTRACT

Neem (*Azadirachta indica A. Juss.*) oil is a renewable feedstock for eco-friendly coatings due to its high oxidative stability and bioactive content. Its industrial adoption in sub-Saharan Africa is limited by low extraction efficiency and variable quality. This study optimized oil recovery using a locally developed semi-automated expeller integrating microwave-assisted pre-treatment with mechanical pressing. A Box–Behnken design within Response Surface Methodology assessed the influence of moisture content (4–12%), microwave duration (2–4 min), feed rate (10–20 kg/h), and screw speed (20–60 rpm) on yield and oil quality. Models exhibited excellent predictive accuracy ($R^2 > 0.99$, $p < 0.0001$), identifying optimal conditions of 7.23% moisture, 2.93 min microwave exposure, 14.68 kg/h feed rate, and 39.65 rpm screw speed, producing 40.43% oil. The extracted oil demonstrated low acid (3.29 mg KOH/g) and peroxide values (2.25 meq O_2/kg), moderate iodine value (83.0 g I_2/100 g), high oxidative stability (6.5 h), thermal resistance (248.5°C), and retained unsaturated and bioactive compounds. The process improved yield, energy efficiency, and processing time, highlighting neem oil's suitability for sustainable coatings and circular bioeconomy applications.

Keywords: Neem Oil, Process Optimization, Semi-Automated Screw Expeller, Microwave Pre-Treatment, Sustainable Coatings

1. INTRODUCTION

The global transition toward a circular bioeconomy and low-carbon manufacturing has intensified the search for renewable feedstocks in engineering applications, particularly in surface coatings, adhesives, and polymeric binders. Vegetable oils have emerged as viable substitutes for petroleum-derived resins due to their biodegradability, low toxicity, and reduced volatile organic compound (VOC) emissions, thereby addressing increasingly stringent environmental and regulatory requirements in coating technologies (Calovi et al., 2024; Santos et al., 2024).

Neem (Azadirachta indica A. Juss.) seed oil is a non-edible and underutilized bio-resource with considerable industrial potential. Its fatty acid composition, primarily oleic (25–54%), linoleic (6–16%), palmitic (16–34%), and stearic (9–24%) acids, supports oxidative crosslinking and polymerization, making it suitable for alkyd, epoxy, and polyurethane resin systems (Biswas

Publisher
Faculty of Engineering and Technology,
Kwara State University, Malete. P.M.B. 1530 Ilorin,
Kwara State, Nigeria.

https://doi.org/10.5281/zenodo.21704339

et al., 2002; Ramadan, 2023). In addition to its lipid profile, neem oil contains bioactive limonoids, including azadirachtin, nimbin, and salannin, which confer antimicrobial and insect-repellent properties, thereby extending its applicability to protective and functional coatings (Isman, 2015; Schmutterer, 1990).

The concentration and stability of azadirachtin and related phytochemicals are critical determinants of neem oil quality and performance, particularly in high-value industrial and agricultural applications (Baby et al., 2022). However, these constituents are highly sensitive to factors such as botanical origin, seed maturity, storage conditions, and extraction technique (Cabral et al., 2023). Consequently, neem oil should not be regarded as a uniform material but rather as a variable system whose physicochemical properties depend strongly on pre- and post-harvest handling as well as processing conditions. In this study, the plant material was botanically authenticated as Azadirachta indica A. Juss., and a voucher specimen was deposited in the Department of Plant Biology, Kwara State University, Malete, Nigeria, to ensure traceability and reproducibility.

Despite its abundance in sub-Saharan Africa and South Asia, neem oil remains underutilized at the industrial scale due to inefficient extraction techniques, inconsistent product quality, and limited process optimization. Conventional mechanical pressing methods typically yield less than 25% oil recovery and are often associated with elevated acid and peroxide values, which constrain their suitability for high-performance applications (Mohd et al., 2022; Özturk et al., 2020). Moreover, critical oil quality parameters such as acid value, iodine value, peroxide value, and bioactive retention are strongly influenced by processing conditions but are rarely optimized simultaneously with oil yield.

Microwave-assisted pre-treatment coupled with screw-type mechanical pressing has demonstrated potential for enhancing oil recovery, reducing processing time, and improving extraction efficiency (Azadbakht et al., 2020; Azadmard-Damirchi et al., 2010; Gai et al., 2013; Zhou et al., 2016). The mechanism involves rapid volumetric heating, which disrupts cellular structures, reduces oil viscosity, and facilitates oil release during mechanical expression. However, systematic multivariate optimization of such hybrid extraction systems for neem oil remains limited, particularly within the Nigerian context. Statistical tools such as Response Surface Methodology, especially the Box–Behnken Design, provide robust frameworks for modeling nonlinear interactions among process variables and optimizing multiple responses simultaneously.

Accordingly, this study systematically investigates the effects of key processing parameters; moisture content, microwave pre-treatment duration, feed rate, and screw speed, on the yield and quality of neem seed oil extracted using a locally developed semi-automated screw expeller. The extracted oils were characterized based on acid value, iodine value, peroxide value, saponification value, fatty acid composition, and azadirachtin content using standardized analytical protocols. The objective is to establish optimal operating conditions that maximize oil recovery while preserving critical physicochemical and bioactive properties required for downstream engineering applications, particularly sustainable coating systems. The findings are expected to support the development of scalable and energy-efficient neem oil extraction technologies and to enhance the valorization of indigenous bio-resources within emerging green manufacturing systems.

2.0MATERIALS AND METHODS

2.1 Raw Materials

Mature neem (Azadirachta indica A. Juss.) fruits were collected from Kwara State, Nigeria. The plant material was botanically authenticated, and only fully matured fruits were selected to ensure high oil content and compositional consistency. After collection, fruits were manually sorted to remove damaged, immature, and pest-infested samples. The selected seeds were screened for uniform size and initial moisture content to minimize feedstock variability and enhance experimental reproducibility.

Neem kernels are known to contain approximately 30–45% oil, with significant levels of bioactive limonoids such as azadirachtin, and a fatty acid profile dominated by C16–C22 components that support oxidative polymerization and film formation in coating applications (Agbo et al., 2019; Arunachalam et al., 2025; Biswas et al., 2002). These characteristics informed their selection for the present study.

2.2 Chemicals and Reagents

All reagents used for physicochemical characterization were of analytical grade. These included ethanol, sodium hydroxide (NaOH), phenolphthalein indicator, hydrochloric acid (HCl), glacial acetic acid, chloroform, potassium iodide (KI), sodium thiosulfate ($Na_2S_2O_3$), and acetic anhydride.

Physicochemical analyses of the extracted oil were conducted in accordance with standardized methods of the AOAC International (AOAC, 2023) and relevant American Oil Chemists' Society procedures, ensuring

consistency and comparability with established oilseed processing studies (Ghosh et al., 2022; Zhou et al., 2016).

2.3 Equipment and Instrumentation

Oil extraction experiments were carried out using a locally developed semi-automated screw press expeller. The system comprised a screw shaft enclosed in a perforated barrel, powered by a variable-speed electric motor and coupled with a speed control unit (Model XSY-ATI-2200X). The expeller was designed to allow independent regulation of screw speed (20–60 rpm) and feed rate (10–20 kg h^{-1}), while kernel feeding was performed manually through a hopper, defining the semi-automated mode of operation. Temperature within the pressing chamber was monitored using an integrated thermal sensor to limit excessive heat buildup and preserve thermolabile constituents.

Kernel moisture content was determined using a digital moisture analyzer (Model BM-50-10, accuracy ±0.01%), given the strong influence of moisture on oil expression efficiency and oxidative stability. Microwave pre-treatment was performed using a laboratory microwave oven operating at a fixed power of 700 W and frequency of 2450 MHz to induce rapid volumetric heating and enhance cellular disruption prior to mechanical pressing. Extracted oil mass was measured using a digital analytical balance (±0.01 g). Where necessary, crude oil samples were centrifuged to remove suspended solids before analysis. Oil yield was calculated as the percentage ratio of extracted oil mass to the initial dry kernel mass, expressed on a dry basis.

2.4 Seed Preprocessing

Harvested neem fruits were depulped manually, washed with clean water, and sun-dried for 5–7 days to reduce moisture content to below 12% (wet basis), which is considered suitable for efficient mechanical oil extraction (Orhevba, 2024). The dried seeds were stored in breathable jute sacks under shaded ambient conditions to minimize moisture reabsorption and microbial deterioration prior to processing.

Before oil extraction, the seeds were mechanically dehulled using a kernel cracker based on the design reported by Opobiyi et al. (2019). The obtained kernels were weighed, visually inspected, and screened to ensure uniformity in size and physical integrity. This preprocessing step was necessary to improve oil recovery efficiency and ensure consistent feeding behavior during mechanical expression.

Figure 1 shows the dried neem seeds after conditioning, while Figure 2 presents the dehulled kernels prepared for oil extraction.

Figure 1: Neem seeds after drying.

Figure 2: Dehulled neem kernels prior to oil extraction.

2.5 Process Parameter Conditioning

Four independent process variables were investigated: moisture content (MC), microwave pre-treatment duration (MD), feed rate (FR), and screw speed (SS). The selected ranges were based on preliminary trials and literature to ensure stable operation and measurable response variation.

Moisture Content Adjustment

Kernel moisture content was conditioned to 4, 8, and 12% (wet basis). For moisture reduction, samples were oven-dried at 105 ± 2 °C until constant mass was achieved. Moisture content was determined using Eq. (1):

$$MC\ (\%) = \frac{W_i - W_f}{W_f} \times 100 \quad (1)$$

Where; W_1 = initial weight (g), W_2 = final weight (g).

where:
Wi=initial mass of sample (g)
Wf = final mass of sample after drying (g)

For moisture increase, a calculated quantity of distilled water was uniformly sprayed onto the kernels and equilibrated in sealed polyethylene
bags for 24 h at ambient temperature. The amount of water added was computed as shown in Eq. (2), following the approach of Martinez et al. (2017):

$$Q = \frac{A(b-a)}{(100-b)} \quad (2)$$

where:
Q = mass of water added (kg)
A = initial mass of kernels (kg)
a = initial moisture content (% wet basis)
b = target moisture content (% wet basis)

Microwave Pre-treatment

Conditioned kernels were subjected to microwave heating at a constant power of 700 W and frequency of 2450 MHz for durations of 2, 3, and 4 min. This range was selected to ensure consistency with the experimental design and to avoid thermal degradation of heat-sensitive bioactive compounds.

Feed Rate and Screw Speed

Feed rate (10–20 kg h^{-1}) was controlled using an adjustable auger mechanism, while screw speed (20–60 rpm) was regulated via a digital speed controller. These parameters were selected based on machine capacity and operational stability limits.

2.6 Oil Extraction Procedure and Energy Analysis

Conditioned neem kernels were processed using the semi-automated screw press expeller (Fig. 3). During operation, the pressing chamber temperature was maintained between 50 and 60 °C to enhance oil flow while minimizing thermal degradation of oil quality attributes.

The expressed crude oil (Fig. 4) was collected, filtered through muslin cloth, and weighed using a digital analytical balance (±0.01 g). Oil yield was calculated on a dry basis as expressed using in Eq. (3):

$$\text{Oil Yield}\,(\%) = \frac{Mo}{Mk} \times 100 \quad (3)$$

where:
Mo = mass of extracted oil (g)
Mk = dry mass of processed kernels (g)

Specific Energy Consumption (SEC)

To evaluate process efficiency, the specific energy consumption was calculated as shown in Eq. (4):

$$SEC = \frac{P \times t}{M_o} \quad (4)$$

where:
SEC = specific energy consumption (kWh kg^{-1} of oil)
P = power rating of the expeller motor (kW)
t = extraction time per batch (h)
Mo = mass of oil produced (kg)

This parameter provides a quantitative measure of energy efficiency and is essential for assessing the feasibility of scale-up and industrial application.

Figure 3: Semi-automated screw press expeller showing: (A) thermal control unit, (B) feed auger, (C) pressing chamber, (D) speed control switch, (E) hopper, (F) twin-head gearbox, and (G) electric motor.

Figure 4: Neem oil obtained after screw press extraction.

2.7 Experimental Design

A Box–Behnken Design (BBD) within the framework of Response Surface Methodology was employed to evaluate the individual and interactive effects of process variables on oil yield and quality responses. The BBD was selected due to its statistical efficiency, reduced number of experimental runs, and suitability for fitting second-order polynomial models (Montgomery, 2019).
Four independent variables were considered: moisture content (X_1), microwave duration (X_2), feed rate (X_3), and screw speed (X_4). Each variable was studied at three coded levels (−1, 0, +1). A total of 25 experimental runs (including one center point) were conducted to ensure adequate estimation of experimental error and model adequacy.
Coding of Variables
The relationship between coded and actual values was expressed as in Eq. 5:

$$X_i = \frac{x_i - x_0}{\Delta x} \quad (5)$$

where:
Xi = coded value of variable
xi = actual value of variable
x_0 = value at center point
Δ_X = step change

Table 1. Experimental ranges and coded levels of independent variables

Variable	Parameter	Unit	−1	0	+1
X_1	Moisture Content	% (w.b.)	4	8	12
X_2	Microwave Duration	Min	2	3	4
X_3	Feed Rate	kg h^{-1}	10	15	20
X_4	Screw Speed	Rpm	20	40	60

Model Development

The experimental data were fitted to a second-order polynomial model as presented in Eq. (6):

$$Y = \beta_0 + \sum \beta_i X_i + \sum \beta_{ii} X_i^2 + \sum \beta_{ij} X_i X_j \quad (6)$$

where:
Y = predicted response
β_0 = intercept term
β_i = linear coefficients
β_{ii} = quadratic coefficients
β_{ij} = interaction coefficients
Xi, Xj = coded independent variables

Model adequacy was evaluated using analysis of variance (ANOVA), including determination of coefficient of determination (R^2), adjusted R^2, coefficient of variation (CV), and lack-of-fit tests at a significance level of $p < 0.05$.

2.8 Oil Characterization

Following extraction, neem oil samples were subjected to comprehensive physicochemical and compositional analyses to evaluate their suitability for bio-based coating applications. All analyses were conducted in triplicate, and results were reported as mean ± standard deviation. Standard analytical procedures of the American Oil Chemists' Society and AOAC International were followed to ensure accuracy, reproducibility, and comparability with existing literature.

2.8.1 Acid Value (AV)

Acid value, which indicates free fatty acid content and the extent of hydrolytic degradation, was determined according to AOCS Cd 3d-63 using ethanolic potassium hydroxide and phenolphthalein indicator. It was calculated as presented in Eq. (7&:

$$AV = \frac{V \times N \times 56.1}{W} \quad (7)$$

where:
AV = acid value (mg KOH g^{-1} oil)
V = volume of KOH used (mL)
N = normality of KOH solution (mol L^{-1})
W = mass of oil sample (g)
56.1 = molecular weight of KOH (g mol^{-1})

2.8.2 *Iodine Value (IV)*

Iodine value, representing the degree of unsaturation, was determined using the Wijs method in accordance with AOCS Cd 1-25. The value was calculated using Eq. (8):

$$IV = \frac{(B - S) \times N \times 12.69}{W} \quad (8)$$

where:
IV = iodine value (g I_2 100 g^{-1} oil)
B = blank titration volume (mL)
S = sample titration volume (mL)
N = normality of sodium thiosulfate (mol L^{-1})
W = mass of oil sample (g)
12.69 = iodine equivalence factor

2.8.3 *Peroxide Value (PV)*

Peroxide value, an indicator of primary oxidation, was determined according to AOCS Cd 8b-90. The value was calculated as shown in Eq. (9):

$$PV = \frac{(S - B) \times N \times 1000}{W} \quad (9)$$

where:
PV = peroxide value (meq O_2 kg^{-1} oil)
S = sample titration volume (mL)
B = blank titration volume (mL)
N = normality of sodium thiosulfate (mol L^{-1})
W = mass of oil sample (g)

2.8.4 *Saponification Value (SV)*

Saponification value was determined in accordance with AOCS Cd 3-25 by refluxing the oil sample with ethanolic KOH followed by back-titration with HCl. It was calculated using Eq. (10):

$$SV = \frac{(B - S) \times N \times 56.1}{W} \quad (10)$$

where:
SV = saponification value (mg KOH g^{-1} oil)
B = blank titration volume (mL)
S = sample titration volume (mL)
N = normality of HCl (mol L^{-1})
W = mass of oil sample (g)

2.8.5 *Kinematic Viscosity*

Kinematic viscosity was measured at 25 °C using a capillary viscometer in accordance with ASTM D445. The viscosity was calculated using Eq. 11:

$$v = k \times t \quad (11)$$

where:
v = kinematic viscosity (m^2 s^{-1})
K = viscometer constant (m^2 s^{-2})
t = flow time (s)

2.8.6 *Oxidative Stability*

Oxidative stability was determined using a Rancimat apparatus according to EN 14112. Approximately 5 g of oil was heated at 130 °C under an oil flow rate of 10 L h^{-1}. The induction period (IP), representing resistance to oxidation, was recorded in hours based on conductivity changes in the measuring vessel.

2.8.7 *Hydroxyl Value (HV)*

Hydroxyl value was determined following AOCS Cd 13-60 using acetylation with acetic anhydride and back-titration with sodium hydroxide. It was calculated using Eq. (12):

$$HV = \frac{(B - S) \times N \times 56.1}{W} \quad (12)$$

where:
HV = hydroxyl value (mg KOH g^{-1} oil)
B = blank titration volume (mL)
S = sample titration volume (mL)
N = normality of NaOH (mol L^{-1})
W = mass of oil sample (g)

2.8.8 *Moisture Content*

Moisture content was determined using a gravimetric oven-drying method (AOAC 925.10). Approximately 5 g of oil was dried at 105 °C for 2 h and calculated using Eq. (13):

$$MC = \frac{W_i - W_f}{W_i} \times 100 \quad (13)$$

where:
MC = moisture content (%)
Wi = initial mass (g)
Wf = final mass after drying (g)

2.8.9 *Thermal Stability*

Thermal stability was evaluated using thermogravimetric analysis (TGA) with a heating rate of 10 °C min^{-1} from 25 to 600 °C under a nitrogen atmosphere. Percentage mass loss was determined as presented in Eq. (14):

$$\text{Mass Loss} = \frac{W_i - W_f}{W_i} \times 100 \quad (14)$$

where:
Wi = initial mass (g)
Wf = final mass at a given temperature (g)

2.8.10 Phytochemical and Fatty Acid Composition

Phytochemical Analysis

Bioactive compounds (azadirachtin A, nimbin, and salannin) were quantified using UV–visible spectrophotometry. Oil samples were dissolved in methanol, filtered (0.45 µm), and analyzed at characteristic wavelengths (214–230 nm). Quantification was performed using calibration curves prepared from certified standards.

Fatty Acid Profile

Fatty acid composition was determined by gas chromatography with flame ionization detection (GC–FID). Oil samples (100 mg) were converted to fatty acid methyl esters (FAMEs) via base-catalyzed transesterification using methanolic KOH. Separation was performed using an HP-88 capillary column (100 m × 0.25 mm × 0.20 µm), with oven temperature programmed from 120 to 230 °C.
Fatty acid composition was calculated using Eq. (15):

$$FA = \frac{\text{Peak area of individual FA}}{\text{Total peak area}} \times 100 \quad (15)$$

where:
FA = fatty acid composition (%)

3.RESULTS AND DISCUSSION

3.1 Experimental Data and Model Adequacy

The experimental design matrix and corresponding responses for neem oil extraction are presented in Table 2. The Box–Behnken Design (BBD) adequately spans the experimental domain of moisture content (X_1, %), microwave pretreatment duration (X_2, min), feed rate (X_3, kg h^{-1}), and screw speed (X_4, rpm), thereby enabling reliable estimation of linear, interaction, and quadratic effects on oil yield (Y_1), acid value (Y_2), iodine value (Y_3), and peroxide value (Y_4).
All experimental runs were conducted in triplicate, and results are reported as mean ± standard deviation (Table 2), ensuring statistical reliability and reproducibility of the semi-automated screw expeller system. The relatively low standard deviations across the responses indicate good process stability and measurement precision.
A multi-response optimization framework based on desirability functions was adopted to simultaneously maximize oil yield and iodine value while minimizing acid value and peroxide value. This approach is consistent with quality-driven optimization strategies widely applied in oilseed processing systems, where both extraction efficiency and product stability must be jointly controlled (Busari et al., 2020; Fadeyibi et al., 2020). Similar approaches have been successfully used to balance competing process objectives in thermomechanical extraction systems.
The adequacy of the developed models was evaluated using analysis of variance (ANOVA), coefficient of determination (R^2), adjusted R^2, predicted R^2, and coefficient of variation (CV), as summarized in Table 3 for oil yield. The high R^2 values obtained (R^2 = 0.9987) indicate that the models explain nearly all variability in the responses, while the close agreement between adjusted and predicted R^2 confirms strong predictive capability without overfitting. Furthermore, the low coefficient of variation (CV = 0.61%) reflects high experimental precision, and the low residual variance demonstrates minimal unexplained error.

Table 2: Box–Behnken Experimental Design Matrix and Measured Responses for Neem Oil Extraction (Mean ± Standard Deviation, N = 3).

Std	Run	X1 (%)	X2 (Min)	X3 (kg/ hr)	X4 (rpm)	Y1 (%)	Y2 (mg KOH g^{-1})	Y3 (g I_2 100 g^{-1})	Y4 (meq O_2 kg^{-1})
5	1	8	3	10	20	34.85 ± 0.12	3.42 ± 0.02	80.12 ± 0.15	2.68 ± 0.03
14	2	8	4	10	40	35.10 ± 0.10	3.45 ± 0.02	80.05 ± 0.14	2.75 ± 0.04
9	3	4	3	15	20	36.20 ± 0.14	3.31 ± 0.01	82.05 ± 0.18	2.42 ± 0.02
17	4	4	3	10	40	36.50 ± 0.13	3.28 ± 0.02	82.40 ± 0.16	2.39 ± 0.03
2	5	12	2	15	40	35.22 ± 0.11	3.49 ± 0.02	79.66 ± 0.12	2.59 ± 0.03
21	6	8	2	15	20	34.98 ± 0.10	3.40 ± 0.02	79.22 ± 0.13	2.64 ± 0.03
13	7	8	2	10	40	35.35 ± 0.12	3.47 ± 0.02	80.05 ± 0.15	2.60 ± 0.02
4	8	12	4	15	40	34.80 ± 0.11	3.55 ± 0.03	78.95 ± 0.14	2.78 ± 0.04
20	9	12	3	20	40	34.65 ± 0.13	3.51 ± 0.02	79.90 ± 0.13	2.62 ± 0.03
8	10	8	3	20	60	33.90 ± 0.12	3.48 ± 0.02	78.95 ± 0.12	2.70 ± 0.03
15	11	8	2	20	40	34.95 ± 0.11	3.44 ± 0.02	79.55 ± 0.14	2.58 ± 0.02
7	12	8	3	10	60	34.30 ± 0.10	3.50 ± 0.02	79.20 ± 0.13	2.73 ± 0.03

Std	Run	X1 (%)	X2 (Min)	X3 (kg/ hr)	X4 (rpm)	Y1 (%)	Y2 (mg KOH g^{-1})	Y3 (g I_2 100 g^{-1})	Y4 (meq O_2 kg^{-1})
3	13	4	4	15	40	36.10 ± 0.13	3.33 ± 0.01	81.55 ± 0.16	2.50 ± 0.02
12	14	12	3	15	60	34.55 ± 0.11	3.52 ± 0.02	79.30 ± 0.14	2.67 ± 0.03
22	15	8	4	15	20	34.70 ± 0.10	3.46 ± 0.02	78.85 ± 0.12	2.80 ± 0.04
10	16	12	3	15	20	34.90 ± 0.12	3.48 ± 0.02	79.45 ± 0.13	2.66 ± 0.03
24	17	8	4	15	60	34.25 ± 0.11	3.49 ± 0.02	78.40 ± 0.12	2.77 ± 0.04
23	18	8	2	15	60	34.65 ± 0.10	3.46 ± 0.02	79.12 ± 0.13	2.63 ± 0.03
25	19	8	3	15	40	40.40 ± 0.15	3.29 ± 0.01	82.60 ± 0.18	2.28 ± 0.02
16	20	8	4	20	40	34.55 ± 0.11	3.53 ± 0.02	78.88 ± 0.12	2.71 ± 0.03
11	21	4	3	15	60	35.35 ± 0.12	3.30 ± 0.01	82.10 ± 0.17	2.35 ± 0.02
18	22	12	3	10	40	35.40 ± 0.11	3.50 ± 0.02	79.65 ± 0.13	2.65 ± 0.03
19	23	4	3	20	40	35.70 ± 0.13	3.32 ± 0.01	82.45 ± 0.18	2.30 ± 0.02
1	24	4	2	15	40	36.45 ± 0.14	3.28 ± 0.01	82.25 ± 0.17	2.33 ± 0.02
6	25	8	3	20	20	34.55 ± 0.11	3.47 ± 0.02	79.15 ± 0.13	2.68 ± 0.03

X1 = Moisture Content, X2 = Microwave Duration, X3 = Feed Rate, X4 = Screw Speed
Y1 = Oil Yield, Y2 = Acid Value, Y3 = Iodine Value, Y4 = Peroxide Value

3.2 Response Surface Analysis for Oil Yield

The statistical significance of the quadratic model developed for oil yield is presented in Table 3. The model is highly significant ($p < 0.0001$), with an F-value of 569.23, indicating a strong relationship between the process variables and oil yield. The low residual mean square (0.0044) further confirms that the model adequately captures the variability in the experimental data.

Among the process variables, moisture content (A) exhibited the most pronounced effect on oil yield ($F = 547.02$, $p < 0.0001$), highlighting its dominant role in oil expression. Appropriate moisture levels promote cell wall softening, matrix swelling, and reduced resistance to oil flow during mechanical compression. However, excessive moisture may hinder oil release by forming emulsified structures that restrict flow pathways, as reported in previous studies on oilseed processing (Bai et al., 2016; Taghvaei et al., 2014).

Microwave pretreatment duration (B), feed rate (C), and screw speed (D) also significantly influenced oil yield ($p < 0.0001$), with F-values of 162.75, 284.92, and 266.19, respectively (Table 3). These parameters collectively define the thermomechanical environment within the screw press, affecting heat transfer, residence time, internal pressure development, and shear-induced rupture of oil-bearing cells (Gai et al., 2013; Wang et al., 2020).

Although screw speed showed a strong main effect, several interaction terms involving screw speed were not statistically significant ($p > 0.05$), suggesting reduced sensitivity beyond certain operational limits. At higher speeds, reduced residence time limits effective oil drainage, leading to decreased extraction efficiency, a trend consistent with findings reported by Mohd et al. (2022).

All quadratic terms (A^2, B^2, C^2, and D^2) were highly significant ($p < 0.0001$), indicating pronounced curvature in the response surface. This confirms that optimum oil yield occurs at intermediate levels of the variables rather than at their extremes, reflecting the competing effects of thermal softening, mechanical compression, and flow resistance.

The developed second-order regression model for oil yield in coded variables is given in Equation (16):

$$Y\_1 = 40.4 - 0.449A - 0.245B - 0.324C - 0.313D + 0.0100AB + 0.0225AC - 0.0000AD + 0.0025BC - 0.0025BD + 0.0725CD - 2.02A^2 - 2.50B^2 - 2.63C^2 - 3.08D^2 \quad (16)$$

Table 3: Analysis of variance (ANOVA) for the quadratic response surface model of neem oil yield, including model adequacy indicators (R^2, adjusted R^2, predicted R^2, and coefficient of variation)

Source	Sum of Squares	Df	Mean Square	F-value	p-value	
Model	35.27	14	2.52	569.23	< 0.0001	Significant
A-Moisture Content	2.42	1	2.42	547.02	< 0.0001	
B-Microwave Duration	0.7203	1	0.7203	162.75	< 0.0001	
C-Feed Rate	1.26	1	1.26	284.92	< 0.0001	
D-Screw Speed	1.18	1	1.18	266.19	< 0.0001	
AB	0.0004	1	0.0004	0.0904	0.7699	
AC	0.0020	1	0.0020	0.4575	0.5141	
AD	0.0000	1	0.0000	0.0000	1.0000	
BC	0.0000	1	0.0000	0.0056	0.9416	
BD	0.0000	1	0.0000	0.0056	0.9416	
CD	0.0210	1	0.0210	4.75	0.0543	
A^2	11.50	1	11.50	2597.79	< 0.0001	

B^2	17.71	1	17.71	4000.59	< 0.0001
C^2	19.46	1	19.46	4397.38	< 0.0001
D^2	26.77	1	26.77	6048.72	< 0.0001
Residual	0.0443	10	0.0044		
R^2	0.9987	—	—	—	—
Adj R^2	0.9968	—	—	—	—
Pred R^2	0.9921	—	—	—	—
CV (%)	0.61	—	—	—	—
R^2	0.9987	—	—	—	—

3.2.1 Influence of Processing Variables on Neem Oil Yield

The interaction effects of process variables on oil yield are illustrated in Figures 5–10, where each response surface represents the combined influence of two variables while the remaining factors are held at their central levels. The surfaces exhibit pronounced nonlinear trends, reflecting the coupled thermal and mechanical mechanisms governing oil expression.

The interaction between moisture content and microwave duration (Figure 5) shows a clear optimum region around 8–9% moisture and approximately 3 min microwave exposure. Moderate moisture enhances cellular permeability and oil mobility, while microwave pretreatment weakens cell structures and reduces oil viscosity. However, excessive moisture or prolonged microwave exposure reduces oil yield due to emulsion formation and localized overheating, consistent with observations by Cao et al. (2020) and Wang et al. (2020).

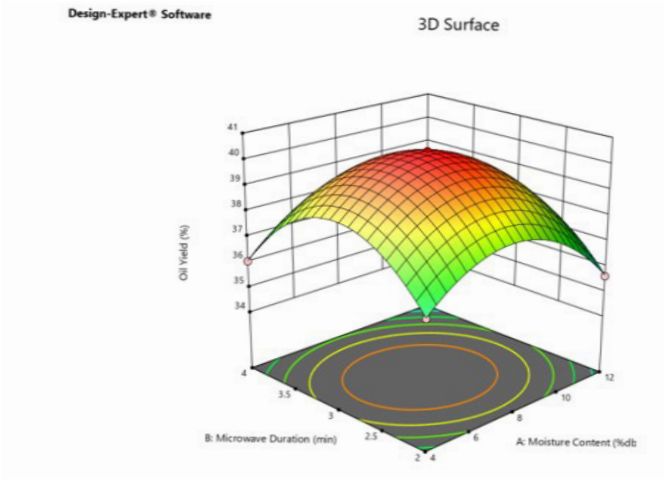

Figure 5: Response Surface Showing the Combined Effects of Moisture Content and Microwave Duration on Neem Oil Yield.

The combined effect of moisture content and feed rate (Figure 6) indicates that maximum oil recovery occurs at moderate feed rates (13–15 kg h^{-1}). Higher feed rates reduce residence time and limit oil expulsion, whereas very low feed rates promote excessive compaction and potential oil reabsorption. This trade-off between throughput and compression has been widely reported in continuous screw press systems (Karaj & Müller, 2011).

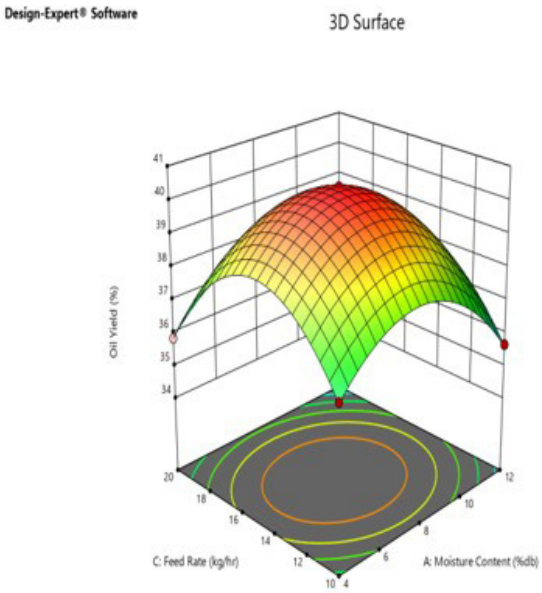

Figure 6: Response Surface Illustrating the Interaction between Feed Rate and Moisture Content on Oil Yield

The interaction between screw speed and moisture content (Figure 7) demonstrates that oil yield decreases with increasing screw speed, particularly at higher moisture levels. Lower screw speeds enhance residence time and compression efficiency, leading to improved oil recovery. Similar findings have been reported for castor and jatropha oil extraction systems (Busari et al., 2022; Savoire et al., 2013).

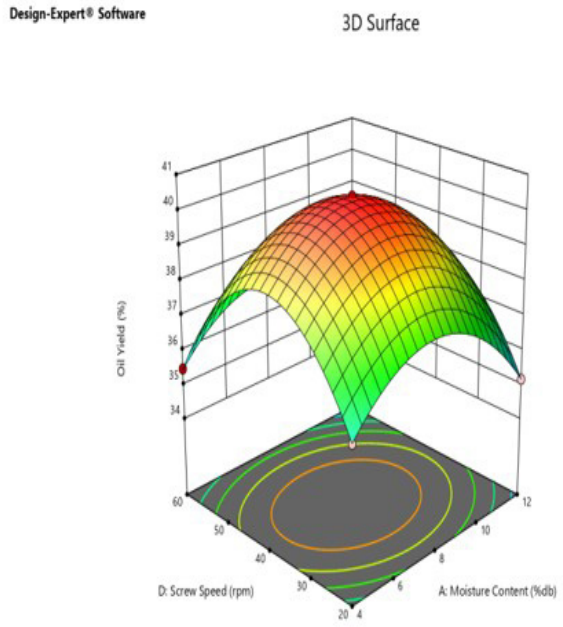

Figure 7: Response Surface Showing the Interaction between Screw Speed and Moisture Content on Oil Yield

As shown in Figure 8, microwave duration and feed rate exhibit a synergistic interaction. Optimal oil yield is achieved at moderate microwave exposure combined with controlled feed rate, where thermal softening facilitates oil release while adequate residence time ensures effective extraction. Excessive heating at high feed rates may result in uneven temperature distribution and reduced efficiency.

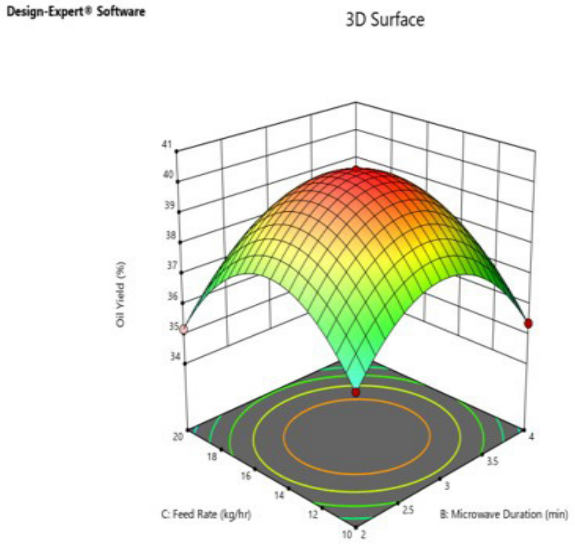

Figure 8: Response Surface Illustrating the Interaction between Microwave Duration and Feed Rate on Oil Yield

The interaction between microwave duration and screw speed (Figure 9) further highlights the importance of thermal–mechanical coupling. Increased microwave exposure combined with lower screw speeds enhances oil recovery by promoting structural breakdown and allowing sufficient time for oil drainage. Comparable behavior has been reported in palm kernel oil extraction (Yusof et al., 2017).

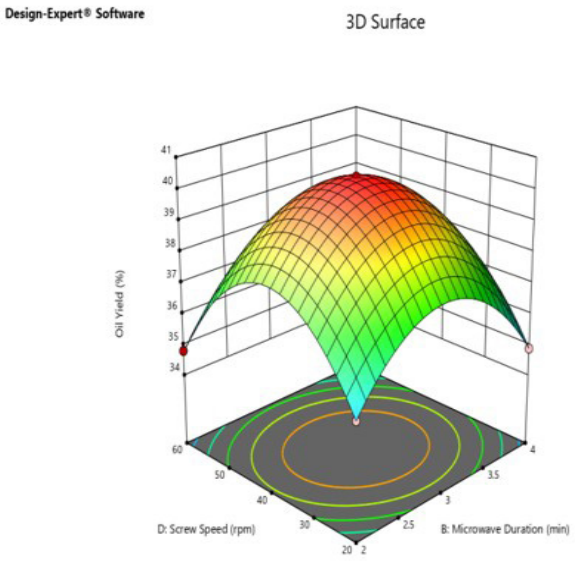

Figure 9: Response Surface Showing the Combined Effects of Microwave Duration and Screw Speed on Oil Yield

The combined effect of feed rate and screw speed (Figure 10) indicates that oil yield is maximized at moderate feed rates and relatively low screw speeds. Increasing screw speed reduces extraction efficiency due to insufficient pressing time, while excessively low feed rates may lead to excessive internal pressure and hinder oil flow. These results emphasize the need for balanced operating conditions to achieve optimal extraction performance.

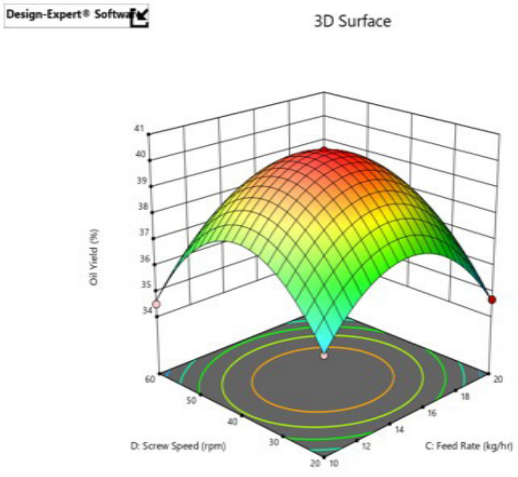

Figure 10: Response Surface Illustrating the Interaction between Feed Rate and Screw Speed on Oil Yield

Model adequacy was further validated using the parity plot shown in Figure 11, where predicted oil yield values are plotted against experimental values. The close clustering of data points along the 45° line indicates strong agreement between model predictions and experimental observations. The random distribution of residuals and high coefficient of determination further confirm the robustness and predictive reliability of the developed model.

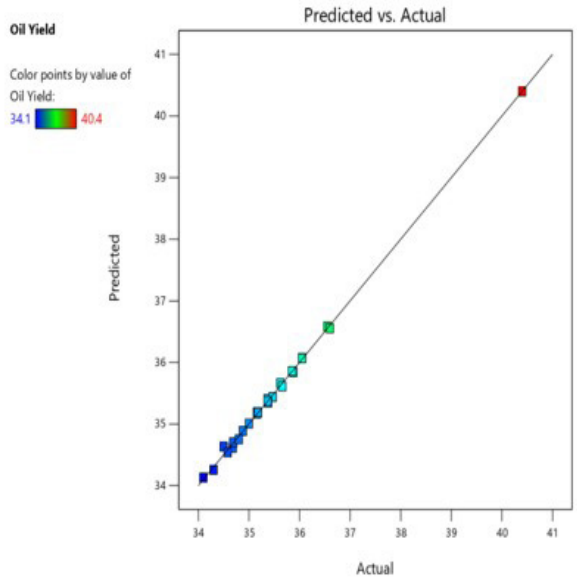

Figure 11: Parity Plot Comparing Experimental and Predicted Oil Yield Values for Neem Oil Extraction Model

3.3 Modelling and Statistical Evaluation of Neem Oil Acid Value

The acid value (AV), which quantifies the concentration of free fatty acids formed through triglyceride hydrolysis, is a critical indicator of oil degradation and directly influences storage stability and suitability for coating formulations. The response was modeled using a second-order polynomial within the framework of Response Surface Methodology, enabling evaluation of both individual and combined effects of the processing variables.

The analysis of variance (ANOVA) results for acid value are presented in Table 4, where the quadratic model is shown to be highly significant ($p < 0.0001$), with a large F-value of 1913.97. This confirms that the selected process variables adequately explain the observed variability in AV. The high coefficient of determination ($R^2 = 0.9996$) indicates that more than 99% of the variation in acid value is captured by the model. Furthermore, the close agreement between the adjusted R^2 (0.9991) and predicted R^2 (0.9982) demonstrates excellent predictive capability and model stability.

The very low residual variance (1.0×10^{-4}) and coefficient of variation (CV = 0.27%) indicate high experimental precision and reliability of the measured data. In addition, the lack-of-fit was not significant ($p > 0.05$), confirming that the model adequately represents the experimental observations within the studied domain.

Among the linear terms, moisture content (A) exerted the most significant effect on acid value ($F = 13440.83$, $p < 0.0001$), followed by microwave duration (B), screw speed (D), and feed rate (C), as shown in Table 4. The positive coefficients for moisture content and microwave duration indicate that increases in these variables promote hydrolytic and thermal degradation, leading to higher free fatty acid formation. In contrast, the negative coefficients associated with feed rate and screw speed suggest that higher throughput conditions reduce acid formation by limiting residence time within the heated press chamber.

All quadratic terms (A^2, B^2, C^2, and D^2) were highly significant ($p < 0.0001$), confirming pronounced curvature in the response surface. This indicates that acid value is highly sensitive to process conditions and that optimal operating regions exist within the experimental domain rather than at extreme parameter values.

Table 4: ANOVA for quadratic model of acid value

Source	Sum of Squares	df	Mean Square	F-value	p-value
Model	0.2680	14	0.0191	1913.97	< 0.0001
A (Moisture)	0.1344	1	0.1344	13440.83	< 0.0001
B (Microwave)	0.0070	1	0.0070	700.83	< 0.0001
C (Feed rate)	0.0014	1	0.0014	140.83	< 0.0001
D (Screw speed)	0.0044	1	0.0044	440.83	< 0.0001
AB	0.0000	1	0.0000	0.00	1.0000
AC	0.0000	1	0.0000	2.50	0.1449
AD	0.0000	1	0.0000	0.00	1.0000
BC	0.0000	1	0.0000	0.00	1.0000
BD	0.0000	1	0.0000	2.50	0.1449

Source	Sum of Squares	df	Mean Square	F-value	p-value
CD	0.0000	1	0.0000	0.00	1.0000
A^2	0.0012	1	0.0012	117.70	< 0.0001
B^2	0.0557	1	0.0557	5567.11	< 0.0001
C^2	0.0444	1	0.0444	4441.23	< 0.0001
D^2	0.0518	1	0.0518	5177.70	< 0.0001
Residual	0.0001	10	0.0000	—	—
Lack-of-fit	(ns)	—	—	—	> 0.05
R^2	0.9996	—	—	—	—
Adj R^2	0.9991	—	—	—	—
Pred R^2	0.9982	—	—	—	—
CV (%)	0.27	—	—	—	—

The developed regression model for acid value in coded variables is expressed in Equation (17):

AV=3.31+0.1058A+0.0242B-0.0108C-0.0192D-0.0025AC-0.0025BD+0.0204A^2+0.1404B^2+0.1254C^2+0.1354D^2 (17)

The dominance of the quadratic coefficients, particularly for microwave duration and feed rate, highlights the strong nonlinear behavior of acid value with respect to processing conditions. The relatively small magnitude of interaction terms suggests that the response is primarily governed by individual factor effects, although coupled thermal–mechanical interactions still contribute to overall system behavior.

3.3.1 Influence of Processing Variables on Acid Value

The interaction effects of moisture content, microwave pretreatment duration, feed rate, and screw speed on acid value are illustrated in the three-dimensional response surface plots presented in Figures 12–17. These plots provide insight into the combined thermal and mechanical mechanisms governing hydrolytic degradation during oil extraction.

The interaction between moisture content and microwave duration (Figure 12) reveals a pronounced increase in acid value with simultaneous increases in both variables. Elevated moisture levels enhance molecular mobility and facilitate hydrolytic cleavage of triglycerides, while microwave heating accelerates thermal degradation reactions. The combined hydrothermal effect promotes the formation of free fatty acids, consistent with earlier findings reported for thermally processed vegetable oils (Zhang et al., 2019; Zhuang et al., 2022)

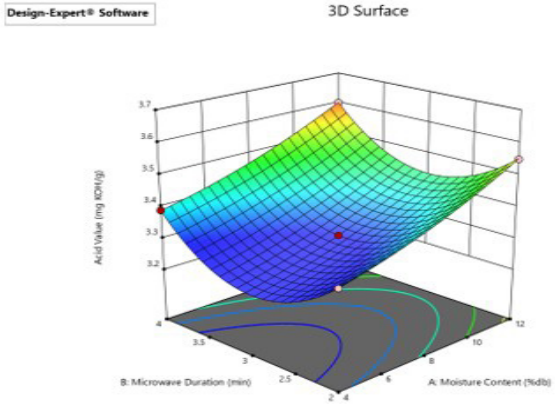

Figure 12: Response surface plot showing the effect of microwave duration and moisture content on acid value

The combined effect of feed rate and moisture content (Figure 13) shows that increasing feed rate reduces acid value, particularly at higher moisture levels. Lower feed rates increase the residence time of the material within the heated barrel, leading to prolonged exposure to heat and moisture and thereby enhancing hydrolytic degradation. In contrast, higher feed rates limit residence time and reduce the extent of degradation, a trend also reported in screw press extraction of oilseeds (Bogaert et al., 2020; Cravotto et al., 2023).

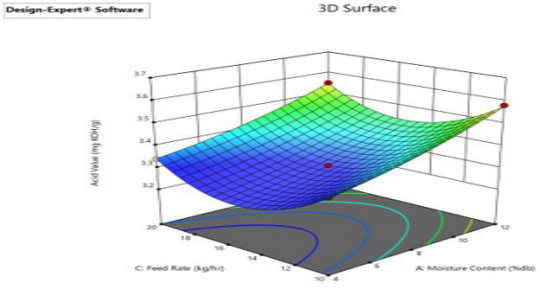

Figure 13: Response surface plot showing the effect of feed rate and moisture content on acid value

As shown in Figure 14, acid value decreases with increasing screw speed, especially at elevated moisture levels. Higher screw speeds facilitate rapid oil discharge and reduce thermal exposure, thereby limiting hydrolysis. This protective effect of increased rotational speed has been previously observed in mechanical oil expression systems (Sharma and Prasad, 2001).

In Figure 14, acid value decreases with increasing screw speed but increases with rising moisture content. Higher screw speeds reduce the residence time and lower the risk of oil degradation by quickly expelling the oil from the pressing chamber (Sharma and Prasad, 2001). This protective effect is especially important at high moisture levels where the potential for hydrolysis is greater.

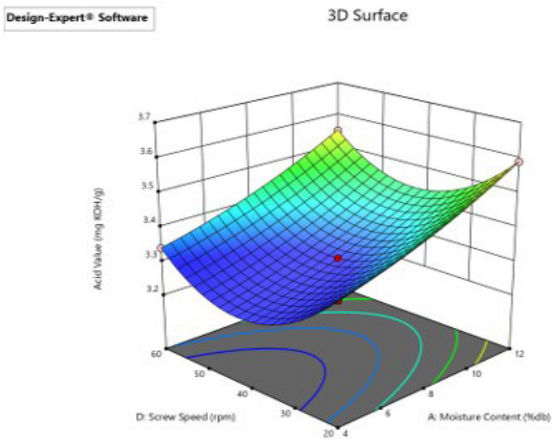

Figure 14: Response surface plot showing the effect of screw speed and moisture content on acid value

The interaction between microwave duration and feed rate (Figure 15) further highlights the competing effects of thermal intensity and residence time. Acid value increases with prolonged microwave exposure but decreases with increasing feed rate. Extended heating enhances lipid oxidation and hydrolysis, while higher feed rates mitigate these effects by shortening exposure time, in agreement with observations by Radočaj et al. (2014).

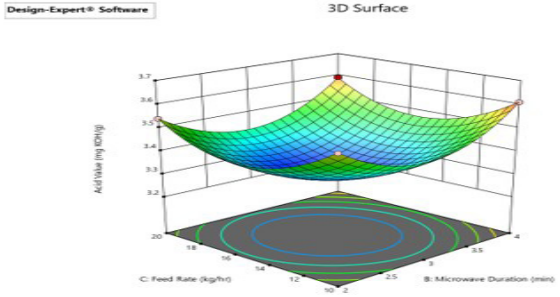

Figure 15: Response surface plot showing the effect of feed rate and microwave duration on acid value

The combined influence of microwave duration and screw speed (Figure 16) demonstrates that increasing screw speed can offset the adverse effects of prolonged microwave exposure. Faster oil discharge reduces the duration of heat–moisture interaction, thereby suppressing acid formation even under extended thermal pretreatment conditions.

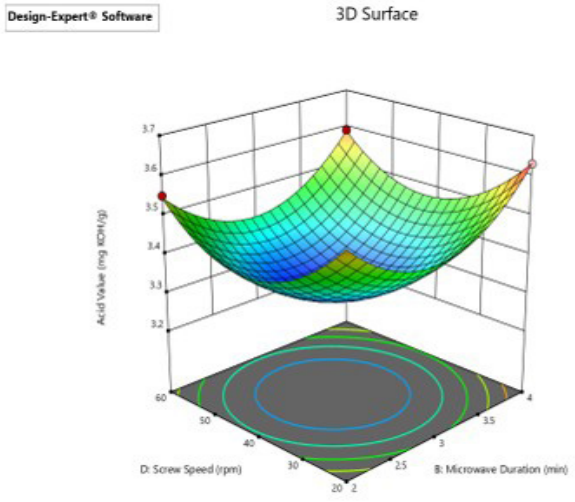

Figure 16: Response surface plot showing the effect of screw speed and microwave duration on acid value

The interaction between feed rate and screw speed (Figure 17) indicates that acid value is minimized at higher levels of both variables. This behavior reflects the importance of mechanical dynamics in controlling degradation, as increased throughput and rapid discharge limit the residence time and reduce exposure to conditions that favor hydrolysis and oxidation (Bakili et al., 2025; Bogaert et al., 2020)..

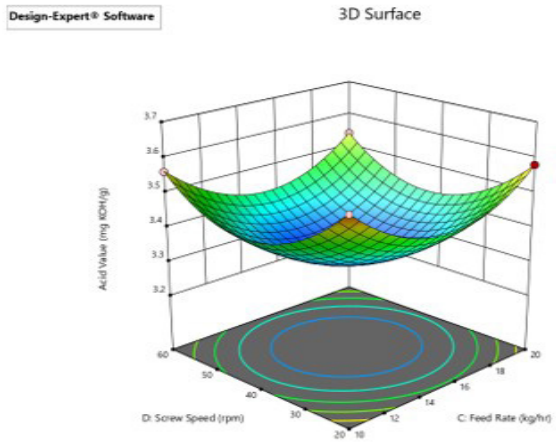

Figure 17: Response surface plot showing the effect of screw speed and feed rate on acid value

Overall, the response surfaces confirm that acid value is primarily governed by hydrothermal exposure and residence time within the extraction system. Minimization of acid value therefore requires operating at moderate moisture levels, short microwave durations, and relatively high feed rate and screw speed to reduce degradation while maintaining extraction efficiency.

Model Validation for Acid Value

The parity plot in Figure 18 demonstrates a strong linear relationship between predicted and actual acid values, with minimal dispersion around the 45° line. This alignment validates the adequacy and predictive power of the quadratic regression model developed. The model's high R^2 value, low residuals, and narrow confidence intervals further confirm its reliability. As such, the model can be confidently used to optimize process parameters in order to achieve desirable acid value levels in neem oil.

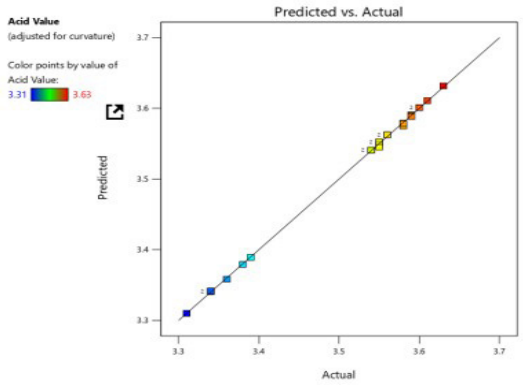

Figure 18: Parity plot comparing predicted and experimental acid values

3.4 Modelling and Statistical Evaluation of Neem Oil Iodine Value

The iodine value (IV) represents the degree of unsaturation in neem oil and is a critical determinant of its drying characteristics and reactivity in coating formulations. Oils with higher iodine values contain a greater proportion of unsaturated fatty acids, which enhances oxidative crosslinking during film formation, thereby improving coating performance (Gunstone, 2004). In this study, iodine value was modeled using a second-order polynomial within the framework of Response Surface Methodology.

The ANOVA results presented in Table 5 confirm that the quadratic model for iodine value is highly significant ($F = 1775.32$, $p < 0.0001$), indicating that the selected process variables adequately describe the response. The coefficient of determination ($R^2 = 0.9996$) shows that over 99% of the variability in iodine value is explained by the model. The adjusted R^2 (0.9990) and predicted R^2 (0.9975) are in close agreement, confirming strong predictive capability and model reliability. The low residual mean square (0.0021) and coefficient of variation (CV = 0.18%) further demonstrate high experimental precision. In addition, the lack-of-fit was not significant ($p > 0.05$), indicating that the developed model adequately represents the experimental data.

Table 5: ANOVA for quadratic model of iodine value

Source	Sum of Squares	df	Mean Square	F-value	p-value
Model	51.74	14	3.70	1775.32	< 0.0001
A (Moisture)	16.08	1	16.08	7723.46	< 0.0001
B (Microwave)	2.77	1	2.77	1332.78	< 0.0001
C (Feed rate)	0.1474	1	0.1474	70.81	< 0.0001
D (Screw speed)	0.1657	1	0.1657	79.59	< 0.0001
AB	0.0056	1	0.0056	2.70	0.1312
AC	0.0000	1	0.0000	0.00	1.0000
AD	0.0000	1	0.0000	0.00	1.0000
BC	0.0000	1	0.0000	0.01	0.9149
BD	0.0056	1	0.0056	2.70	0.1312
CD	0.0000	1	0.0000	0.00	1.0000
A^2	0.0006	1	0.0006	0.27	0.6132 (ns)
B^2	12.05	1	12.05	5788.58	< 0.0001
C^2	6.64	1	6.64	3189.00	< 0.0001
D^2	13.49	1	13.49	6480.60	< 0.0001
Residual	0.0208	10	0.0021	—	—
Lack-of-fit	(ns)	—	—	—	> 0.05
R^2	0.9996	—	—	—	—
Adj R^2	0.9990	—	—	—	—
Pred R^2	0.9975	—	—	—	—
CV (%)	0.18	—	—	—	—

The coded regression model for iodine value is presented in Eq. (18):

IV=82.77-1.16A-0.4808B+0.1108C+0.1175D-0.0375AB-0.0025BC-0.0375BD+0.0142A^2-2.07B^2-1.53C^2-2.19D^2 (18)

The negative linear coefficients for moisture content and microwave duration indicate that increasing either parameter leads to a reduction in iodine value, while positive coefficients for feed rate and screw speed suggest improved preservation of unsaturation under higher throughput conditions. The pronounced negative quadratic coefficients for microwave duration, feed rate, and screw speed confirm strong curvature, indicating that excessive processing intensity accelerates degradation of unsaturated fatty acids.

3.4.1 Influence of Processing Variables on Iodine Value

The iodine value is highly sensitive to both thermal and mechanical processing conditions, as it reflects the stability of carbon–carbon double bonds within fatty acid chains. The interaction between moisture content and microwave duration (Figure 19) shows a clear decline in iodine value with increasing levels of both variables. This behaviour is attributed to hydrothermal degradation, where elevated moisture promotes hydrolysis and facilitates oxidative reactions under thermal conditions, leading to the breakdown of unsaturated bonds (Ghoshal & Sandal, 2024). Prolonged microwave exposure further intensifies molecular agitation and accelerates oxidative degradation, resulting in reduced iodine value.

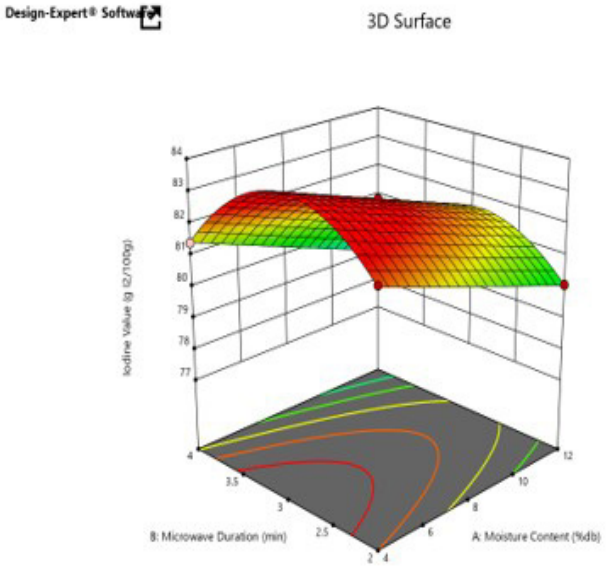

Figure 19: Response surface plot showing the effect of microwave duration and moisture content on iodine value

The interaction between feed rate and moisture content (Figure 20) indicates that iodine value decreases with increasing moisture but improves slightly at higher feed rates. This trend highlights the role of residence time, where higher feed rates reduce exposure to heat and oxygen, thereby preserving unsaturation. Similar observations have been reported in continuous oil expression systems, where reduced residence time minimizes oxidative degradation (Savoire et al., 2013).

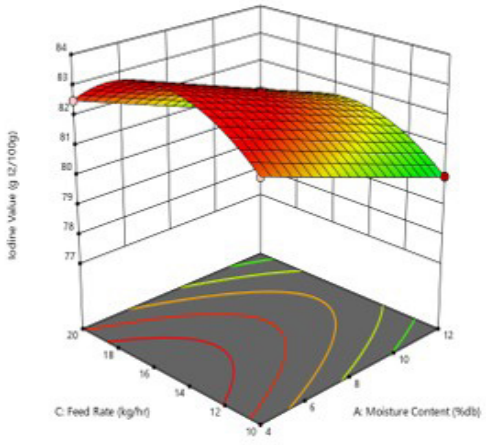

Figure 20: Response surface plot showing the effect of feed rate and moisture content on iodine value

The combined effect of screw speed and moisture content (Figure 21) shows that iodine value improves moderately with increasing screw speed but decreases significantly with higher moisture levels. Increased screw speed facilitates rapid oil discharge, limiting thermal exposure and oxidation. However, at elevated moisture levels, hydrolytic reactions dominate, reducing the effectiveness of this protective mechanism.

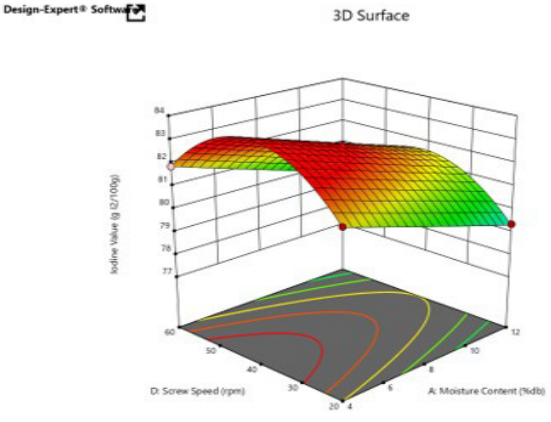

Figure 21: Response surface plot showing the effect of screw speed and moisture content on iodine value

Figure 22 illustrates the interaction between microwave duration and feed rate. Iodine value declines with increasing microwave exposure, while higher feed rates mitigate this reduction by shortening residence time. This demonstrates that controlled material flow can partially offset the adverse effects of thermal processing on unsaturation.

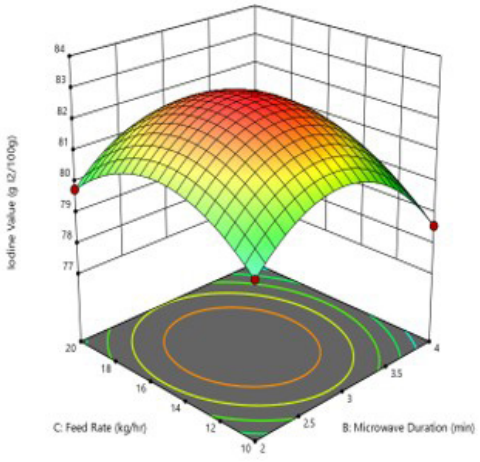

Figure 22: Response surface plot showing the effect of feed rate and microwave duration on iodine value

The interaction between microwave duration and screw speed (Figure 23) further emphasizes the balance between thermal and mechanical influences. While prolonged microwave exposure reduces iodine value, higher screw speeds help preserve unsaturation by accelerating oil extraction and minimizing heat–oxygen interaction.

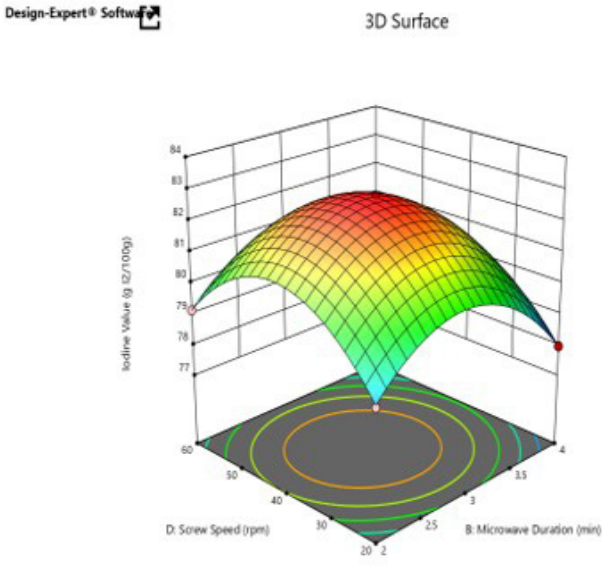

Figure 23: Response surface plot showing the effect of screw speed and microwave duration on iodine value

The relationship between feed rate and screw speed (Figure 24) indicates that iodine value increases with both variables, confirming that rapid extraction conditions favor the retention of unsaturated fatty acids. This aligns with established findings that minimizing thermal residence time is essential for preserving oil quality (Zhuang et al., 2022).

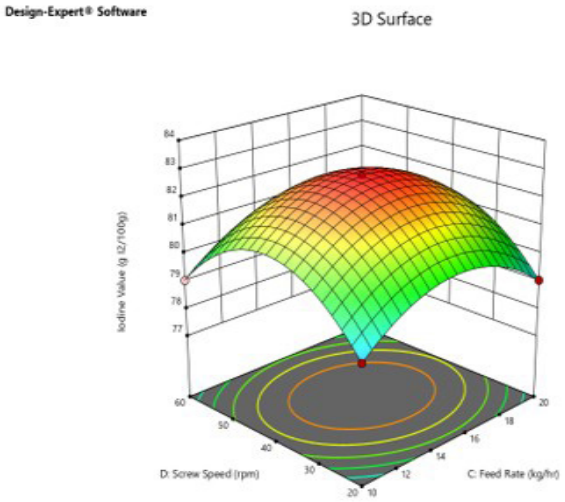

Figure 24: Response surface plot showing the effect of screw speed and feed rate on iodine value

Model Validation for Iodine Value

The adequacy of the developed model was validated using a parity plot (Figure 25), which compares predicted and experimental iodine values. The close alignment of data points along the 45° line indicates strong agreement between predicted and observed values, confirming the reliability and predictive capability of the model. The high coefficient of determination and low residual error further support the robustness of the model for process optimization and scale-up applications.

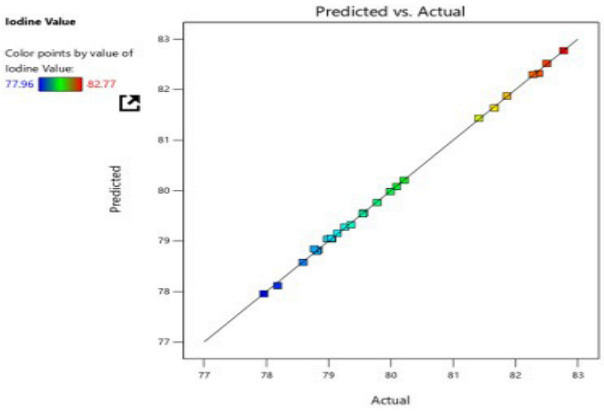

Figure 25: Parity plot comparing predicted and experimental iodine values for the developed model.

3.5 Modelling and Statistical Evaluation of Neem Oil Peroxide Value

Peroxide value (PV) quantifies the concentration of hydroperoxides formed during the early stages of lipid oxidation and is a primary indicator of oxidative stability. In the context of coating and bio-based material applications, low PV is essential to ensure storage stability and prevent premature oxidative degradation prior to film formation (Gomes et al., 2025). In this study, peroxide value was modeled using a second-order polynomial within the framework of Response Surface Methodology.

The ANOVA results presented in Table 6 confirm that the quadratic model is highly significant ($F = 5420.54$, $p < 0.0001$), indicating that the selected process variables adequately explain variations in peroxide value. The coefficient of determination ($R^2 = 0.9999$) shows that nearly all variability in PV is captured by the model. The adjusted R^2 (0.9997) and predicted R^2 (0.9991) are in close agreement, confirming excellent predictive reliability and robustness of the model. The residual mean square (1.0×10^{-5}) is extremely low, while the coefficient of variation (CV = 0.21%) indicates high experimental precision. Furthermore, the lack-of-fit was not significant ($p > 0.05$), confirming that the model adequately represents the experimental data.

Table 6: ANOVA for Quadratic Model of Peroxide Value

Source	Sum of Squares	df	Mean Square	F-value	p-value
Model	0.8221	14	0.0587	5420.54	< 0.0001
A (Moisture)	0.2700	1	0.2700	24923.08	< 0.0001
B (Microwave)	0.1657	1	0.1657	15293.08	< 0.0001
C (Feed rate)	0.0385	1	0.0385	3556.92	< 0.0001
D (Screw speed)	0.0070	1	0.0070	646.92	< 0.0001
AB	0.0000	1	0.0000	0.00	1.0000
AC	0.0000	1	0.0000	0.00	1.0000
AD	0.0000	1	0.0000	0.00	1.0000
BC	0.0000	1	0.0000	2.31	0.1597
BD	0.0000	1	0.0000	0.00	1.0000
CD	0.0000	1	0.0000	2.31	0.1597
A^2	0.0002	1	0.0002	14.66	0.0033
B^2	0.1643	1	0.1643	15169.28	< 0.0001
C^2	0.0792	1	0.0792	7312.40	< 0.0001
D^2	0.1115	1	0.1115	10295.43	< 0.0001
Residual	0.0001	10	0.0000	—	—
Lack-of-fit	(ns)	—	—	—	> 0.05
R^2	0.9999	—	—	—	—
Adj R^2	0.9997	—	—	—	—
Pred R^2	0.9991	—	—	—	—
CV (%)	0.21	—	—	—	—

The coded regression model describing peroxide value is given in Eq. (19):

PV=2.28+0.1500A+0.1175B-0.0567C-0.0242D+0.0025BC+0.0025CD+0.0075A^2+0.2412B^2+0.1675C^2+0.1988D^2 (19)

The positive linear coefficients for moisture content and microwave duration indicate that increasing these parameters promotes peroxide formation, while the negative coefficients for feed rate and screw speed suggest that higher throughput conditions suppress oxidation. The large positive quadratic coefficient associated with microwave duration confirms its dominant role in accelerating oxidative degradation under prolonged exposure, highlighting the sensitivity of neem oil to thermal treatment.

3.5.1 Influence of Processing Variables on Peroxide Value

Peroxide value is strongly governed by the combined effects of thermal intensity, moisture content, and mechanical residence time during oil extraction. The interaction between moisture content and microwave duration (Figure 26) shows a pronounced increase in PV with increasing levels of both variables. This behaviour is attributed to hydrothermal oxidation mechanisms,

where moisture facilitates hydrolytic cleavage of triglycerides and enhances the formation of reactive oxygen species under elevated temperature conditions. Prolonged microwave exposure further intensifies molecular agitation and oxygen diffusion, accelerating hydroperoxide formation.

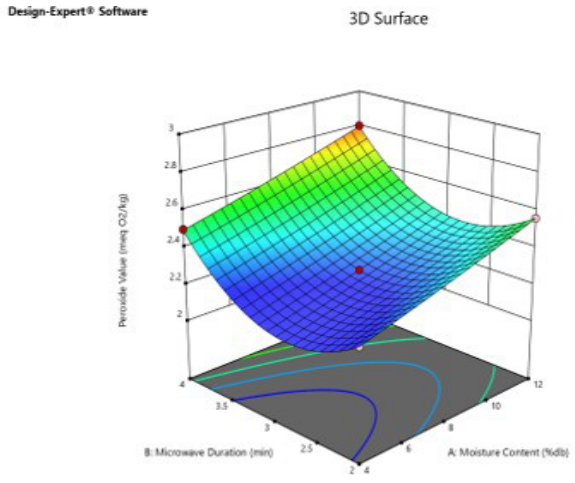

Figure 26: Effect of microwave duration and moisture content on peroxide value

The interaction between feed rate and moisture content (Figure 27) indicates that peroxide value increases with moisture content but decreases at higher feed rates. This reflects the influence of residence time, where lower feed rates prolong exposure to heat and oxygen, thereby promoting oxidation. In contrast, higher feed rates reduce residence time and limit oxidative reactions, consistent with established observations in continuous oil expression systems (Savoire et al., 2013).

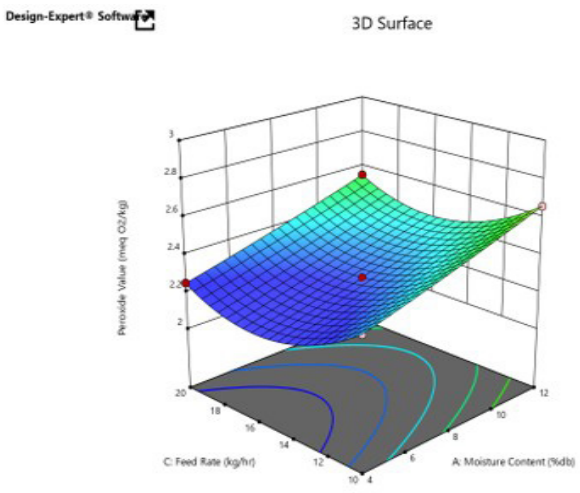

Figure 27: Effect of feed rate and moisture content on peroxide value

The combined effect of screw speed and moisture content (Figure 28) shows that increasing screw speed reduces peroxide value, particularly at lower moisture levels. Higher rotational speeds facilitate rapid oil discharge, minimizing thermal exposure and limiting oxidation. However, at elevated moisture levels, hydrolytic reactions dominate and partially offset the protective effect of increased screw speed.

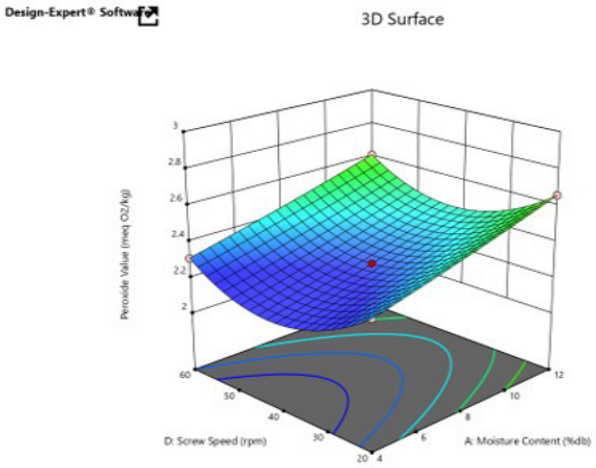

Figure 28: Effect of screw speed and moisture content on peroxide value

Figure 29 illustrates the interaction between feed rate and microwave duration. Peroxide formation is highest at long microwave durations combined with low feed rates, due to prolonged thermal and oxidative exposure. Increasing feed rate mitigates this effect by reducing processing time, thereby limiting the extent of oxidation.

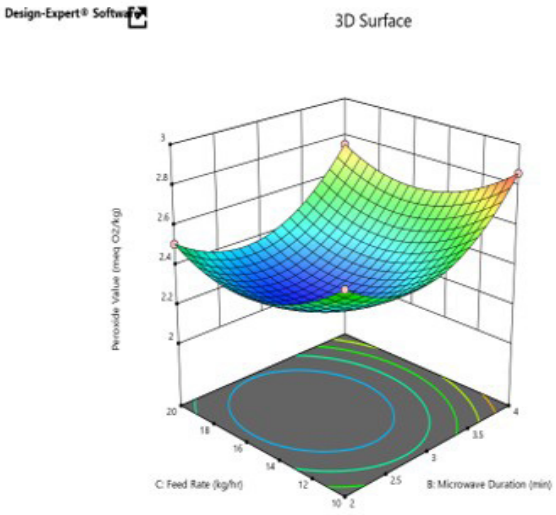

Figure 29: Effect of feed rate and microwave duration on peroxide value

The interaction between screw speed and microwave duration (Figure 30) further highlights the importance of thermal–mechanical balance. High microwave exposure combined with low screw speed results in significant peroxide formation due to extended heating periods. Increasing screw speed reduces this effect by shortening residence time and accelerating oil removal.

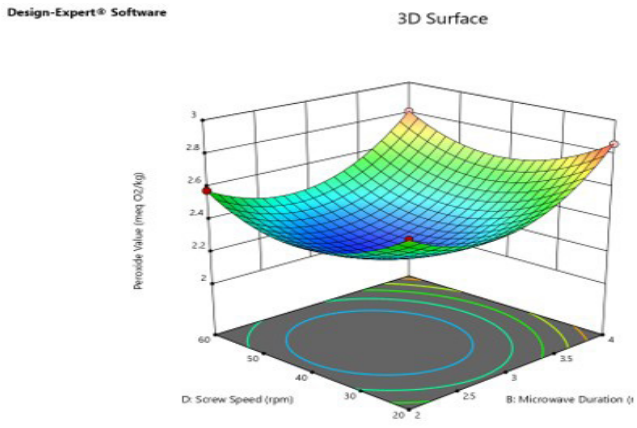

Figure 30: Effect of screw speed and microwave duration on peroxide value

The relationship between feed rate and screw speed (Figure 31) indicates that peroxide value decreases with simultaneous increases in both variables. This synergistic effect is attributed to reduced thermal residence time and rapid oil discharge, which minimize exposure to oxidative conditions and preserve oil quality.

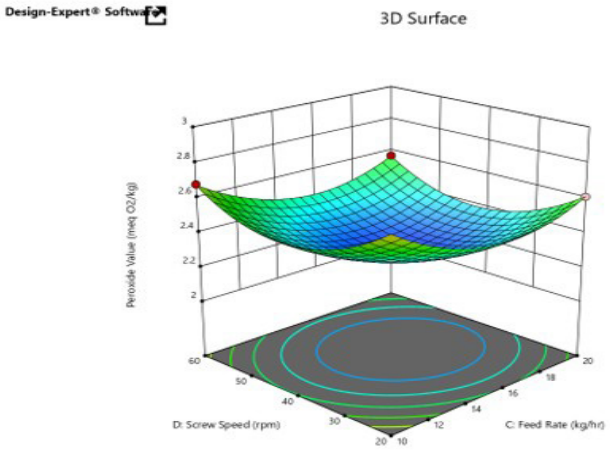

Figure 31: Effect of screw speed and feed rate on peroxide value

Model Validation for Peroxide Value

Model adequacy was validated using a parity plot (Figure 32), which compares predicted and experimental peroxide values. The close alignment of data points along the 45° line indicates strong agreement between predicted and observed values, confirming the accuracy and predictive capability of the developed model. The extremely high coefficient of determination ($R^2 = 0.9999$) and minimal residual deviations further demonstrate that the model effectively captures the nonlinear interactions governing peroxide formation during neem oil extraction.

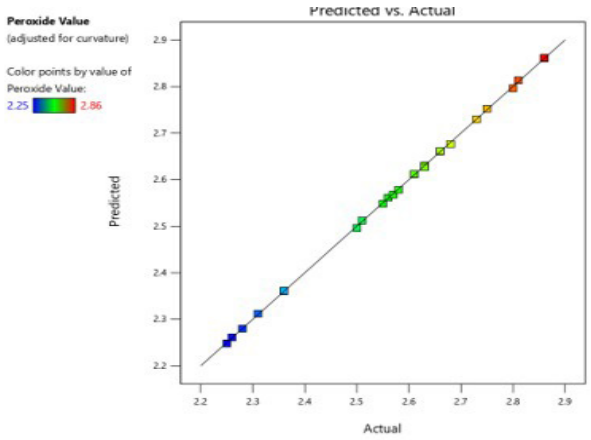

Figure 32: Parity plot comparing predicted and experimental peroxide values for the developed model.

3.6 Optimum operational conditions for neem oil extraction

Response Surface Methodology (RSM) based on a Box–Behnken Design (BBD) was employed to quantify the combined effects of moisture content, microwave pre-treatment duration, feed rate, and screw speed on neem oil yield and associated quality attributes. The developed quadratic models for oil yield, acid value (AV), iodine value (IV), and peroxide value (PV) demonstrated strong statistical adequacy, as evidenced by high coefficients of determination ($R^2 = 0.9930–0.9999$), low residual errors, and non-significant lack-of-fit. These indicators confirm that the models are robust and suitable for predictive optimization within the defined experimental domain.

Multi-response numerical optimization was carried out using desirability function analysis in Design-Expert® to simultaneously maximize oil yield while minimizing AV and PV and maintaining IV within the desirable range for coating applications. The optimal solution, illustrated in Fig. 33, corresponded to a moisture content of 7.23% (dry basis), microwave duration of 2.93 min, feed rate of 14.68 kg h^{-1}, and screw speed of 39.65 rpm. Under these conditions, the predicted responses were 40.43% oil yield, 3.29 mg KOH g^{-1} acid value, 83.00 g I_2/100 g iodine value, and 2.25 meq O_2 kg^{-1} peroxide value, indicating that both hydrolytic and oxidative degradation

were effectively minimized while maintaining high extraction efficiency.

Experimental validation conducted in triplicate under these optimal conditions showed close agreement with model predictions, with relative deviations below 5% for all responses. This confirms the reliability and practical applicability of the developed models for process control and scale-up. The optimized acid value reflects low free fatty acid content, which is essential for minimizing side reactions during resin synthesis. The iodine value confirms the semi-drying nature of neem oil, supporting its applicability in oxidative curing systems such as alkyd coatings, while the low peroxide value indicates enhanced oxidative stability during storage and processing. Overall, the optimized conditions provide a balanced thermomechanical environment that maximizes oil recovery without compromising critical quality attributes.

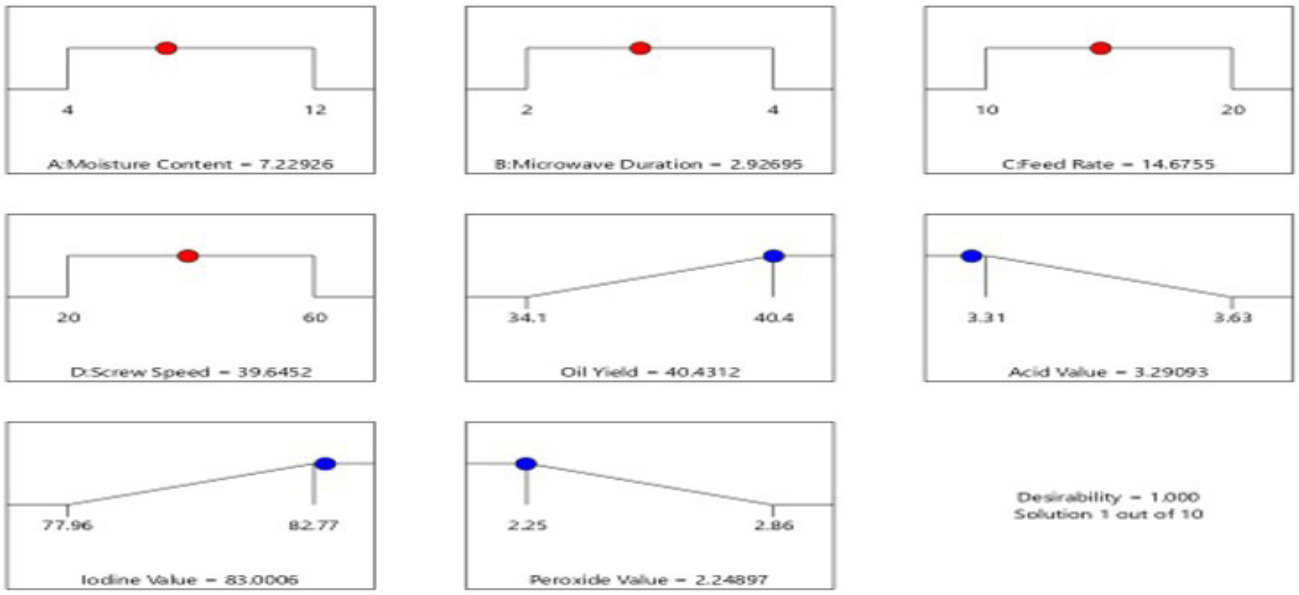

Figure 33: Three-dimensional response surface plots showing the combined effects of moisture content, microwave duration, feed rate, and screw speed on neem oil yield and quality responses.

3.7 Physicochemical and phytochemical characterization of optimized neem oil

Oil extracted under the optimized processing conditions was subjected to detailed physicochemical and compositional analyses to verify its quality, consistency, and suitability for industrial applications. All measurements were conducted in triplicate, and results are presented as mean ± standard deviation. The evaluated parameters included key indicators of oil stability, reactivity, and processing performance, alongside the quantification of major bioactive compounds and fatty acid composition.

The results are summarized in Table 7, while the chemical composition is presented in Table 8.

Table 7: Physicochemical Properties of Neem Oil Extracted Under Optimized Conditions

Parameter	Sample A	Sample B	Sample C	Mean ± SD
Acid value (mg KOH/g)	3.29	3.30	3.29	3.29 ± 0.01
Iodine value (g I_2/100 g)	83.00	82.97	83.08	83.02 ± 0.06
Peroxide value (meq O_2/kg)	2.25	2.25	2.24	2.25 ± 0.01
Saponification value (mg KOH/g)	194.6	195.2	194.8	194.9 ± 0.3
Kinematic viscosity (mm^2/s)	35.6	36.1	35.9	35.9 ± 0.2
Oxidative stability (h)	6.5	6.4	6.3	6.4 ± 0.1
Hydroxyl value (mg KOH/g)	8.2	8.0	8.1	8.1 ± 0.1
Free fatty acid (%)	1.64	1.65	1.64	1.64 ± 0.01
Moisture content (%)	0.28	0.31	0.29	0.29 ± 0.02
Thermal stability (°C)	248.5	249.2	248.8	248.8 ± 0.3

Table 8: Chemical Profile of Neem Oil Extracted Under Optimized Conditions

Constituent	Concentratio
Azadirachtin A	460 ± 12 mg/ kg
Nimbin	205 ± 8 mg/kg
Salannin	150 ± 6 mg/kg
Oleic acid (C18:1)	45.5%
Palmitic acid (C16:0)	16.2%
Stearic acid (C18:0)	12.1%
Linoleic acid (C18:2)	9.8%
Arachidic acid (C20:0)	4.1%

The physicochemical properties presented in Table 7 indicate that the optimized extraction process produced neem oil of high and consistent quality. The acid value remained tightly distributed around 3.29 mg KOH g^{-1}, reflecting minimal hydrolytic degradation and confirming suitability for coating and polymer applications where low free fatty acid content is essential for controlled curing reactions (Das et al., 2021). The iodine value, averaging 83.02 g I_2/100 g, confirms the semi-drying nature of the oil, which is advantageous for oxidative crosslinking in alkyd and related resin systems (Omowanle et al., 2018). Peroxide values were consistently low, indicating that oxidative deterioration during extraction was effectively suppressed.

The saponification value suggests a triglyceride composition favorable for polymer synthesis, while the measured viscosity supports good flow characteristics and uniform film formation during application. Oxidative stability in the range of 6.3–6.5 h indicates resistance to auto-oxidation, which can be attributed to both controlled processing conditions and the presence of natural antioxidants (Sati et al., 2025). The hydroxyl value further highlights the potential for chemical modification, particularly in polyurethane and hybrid resin systems (Gamage et al., 2009). Low moisture content and high thermal stability confirm that the oil is suitable for storage and high-temperature processing without significant degradation.

The compositional analysis in Table 8 reveals that the oil is predominantly composed of oleic acid, reinforcing its classification as a semi-drying oil with favorable film-forming characteristics (Chaudhari et al., 2013). The presence of linoleic acid contributes to curing efficiency, while saturated fatty acids enhance oxidative stability. Importantly, the retention of bioactive limonoids, particularly azadirachtin A, nimbin, and salannin, demonstrates that the integrated microwave-assisted mechanical extraction process preserves functional phytochemicals.

From an industrial perspective, the combination of low degradation indices, moderate unsaturation, and retained bioactivity provides a strong foundation for the development of multifunctional coatings. Compared with conventional extraction methods (Ganorkar et al., 2023; Sati et al., 2025), the optimized process yields oil with improved oxidative stability and comparable or enhanced functional properties. This supports the suitability of neem oil as a sustainable alternative to petroleum-derived feedstocks in coatings, bio-lubricants, and other green material applications, aligning with current advancements in circular bioeconomy systems.

4. CONCLUSION

The following conclusions were drawn from the study:

The integration of microwave-assisted pre-treatment with a semi-automated screw expeller significantly improved neem oil extraction efficiency, demonstrating that controlled thermomechanical processing enhances oil recovery while maintaining desirable physicochemical quality.

Optimal operating conditions (7.23% moisture content, 2.93 min microwave duration, 14.68 kg h^{-1} feed rate, and 39.65 rpm screw speed) produced a maximum oil yield of 40.43% with low acid and peroxide values, moderate iodine value, and good oxidative and thermal stability, confirming suitability for bio-based coating applications.

The developed RSM models exhibited high predictive accuracy and reliability, indicating that moisture content, microwave duration, feed rate, and screw speed must be carefully balanced to maximize oil yield without compromising oil quality and bioactive integrity.

The optimized extraction process shows strong potential for industrial application; however, considerations related to energy consumption and scale-up, including heat distribution and process control, require further investigation.

Future work should focus on pilot-scale validation, detailed energy and economic analysis, and performance evaluation of

neem oil in coating formulations relative to conventional drying oils.

REFERENCES

Agbo, B. E., Nta, A. I., & Ajaba, M. O. (2019). *Bio-pesticidal properties of Neem (Azadirachta indica)* (Vol. 1, pp. 17–26). https://doi.org/10.9734/bpi/atias/v1. https://doi.org/10.9734/bpi/atias/v1

AOAC. (2023). *Official Methods of Analysis of AOAC International (22nd ed.)*. Association of Official Analytical Chemists. https://doi.org/https://doi.org/10.1093/9780197610145.002.001

Arunachalam, B., Ganesan, S., Natarajan, H. P., Suthandhiirajan, R., Muthuswamy, S., Balaiyan, S., & Satheesan, A. (2025). Advancing Neem's role in Environmenal Sustainability: Genetic Potential and Industrial Applications. *Environmental Quality Management*. https://doi.org/https:doi.org/10.1002/tqem.70041

Azadbakht, M., Asadi, G., & Behroozi-Khazaei, N. (2020). Effect of screw press parameters on oil recovery from sunflower seeds. *Biosystems Engineering*, *193*, 1–9. https://doi.org/https://doi.org/10.1016/j.biosystemseng.2020.02.011

Azadmard-Damirchi, S., Habibi-Nodeh, F., Hesari, J., Nemati, M., & Achachlouei, C. (2010). Efffect of pretreatment with microwaves on oxidative stability and nutraceutical content of oil from rapeseed. *Food Chemistry*, *121*(4), 1211–1215. https://doi.org/https://doi.org/10.1016/j.foodchem.2009.12.078

Baby, A. R., Freire, T. B., Marques, G. D., Rijo, P., & Lima, F. V. (2022). Azadirachta indica (Neem) as a Potential Natural Active for Dermocosmetic and Topical Products: A Narrative Review. *Cosmetics*, *9*(3), 58. https://doi.org/https://doi.org/10.3390/cosmetics9030058

Bai, L., Huan, S., Gu, J., & McClements, D. J. (2016). Fabrication of oil-in-water nanoemulsions by dual-channel microfluidization using natural emulsifiers: Saponin, lecithin, and their mixtures. *Food Hydrocolloids*, *61*, 703–711. https://doi.org/https://doi.org/10.1016/j.foodhyd.2016.06.019

Bakili, S., Kivevele, T., Kichonge, B., Salifu, A. A., & King'ondu, C. K. (2025). Furfural from lignocellulose biomass a comprehensive review of hydrolysis methods production technologies and integration into the circular economy. *Discover Sustainability*, *6*(1), 870. https://doi.org/10.1007/s43621-025-01644-5

Biswas, K., Chattopadhyay, I., Banerjee, R. K., & Bandyopadhyay, U. (2002). Biological activities and medicinal properties of neem (Azadirachta indica). *Current Science*, *82*(11), 1336–1345. https://doi.org/http://www.jstor.org/stable/24106000

Bogaert, L., Mhemdi, H., & Vorobiev, E. (2020). Residence time distribution and flow pattern modeling of oilseeds in a pilot screw press. *OCL*, *27*, 65. https://doi.org/10.1051/ocl/2020060

Busari, R. A., Fadeyibi, A., Adebayo, K. R., Oladipupo, R., Muhammed, F. A., & Balogun, R. F. (2020). Process optimization of oil expression from watermelon (Citrullus lanatus) seeds. (Pt. 55–64). *LAUTECH Journal of Engineering and Technology*, *14*(2).

Busari, R. A., Olaoye, J. O., Adebayo, K. R., & Fadeyibi, A. (2022). Development and evaluation of a combined roaster expeller for castor seeds for biodiesel production. *Research in Agricultural Engineering*, *68*(4), 169–179. https://doi.org/https://doi.org/10.17221/83/2020-RAE

Cabral, S. M., Silva, F. L., Rodrigues, P. J., & Diel Rambo, M. K. (2023). Extraction and chemical characterization of neem seed oil (Azadirachta indica). *Journal of Biotechnology and Biodiversity*, *11*(4), 170–181. https://doi.org/10.20873/jbb.uft.cemaf.v11n4.16258

Calovi, M., Zanardi, A., & Rossi, S. (2024). Recent Advances in Bio-Based Wood Protective Systems: A Comprehensive Review. *Applied Sciences*, *14*, 736. https://doi.org/https://doi.org/10.3390/app14020736

Cao, F., Yang, L., & Lu, X. (2020). Effects of processing conditions on the quality of walnut oil. *LWT - Food Science and Technology*, *133*(110089). https://doi.org/https://doi.org/10.1016/j.lwt.2020.110089

Chaudhari, A. B., Anand, A., Rajput, S. D., Kulkarni, R. D., & Gite, V. V. (2013). Synthesis, characterization and application of *Azadirachta indica juss* (neem oil) fatty amides (AIJFA) based polyurethanes coatings: A renewable novel approach. *Progress in Organic Coatings, Coatings Science International 2012*, *76*(12), 1779–1785. https://doi.org/10.1016/j.porgcoat.2013.05.016

Cravotto, C., Claux, O., Bartier, M., Fabiano-Tixier, A.-S., & Tabasso, S. (2023). Leading Edge Technologies and Perspectives in Industrial Oilseed Extraction. *Molecules*, *28*(16), 5973. https://doi.org/10.3390/molecules28165973

Das, P., Sharma, N., Puzari, A., Kakati, D. K., & Devi, N. (2021). Synthesis and characterization of neem (Azadirachta indica) seed oil-based alkyd resins for efficient anticorrosive coating application. *Polymer Bulletin*, *78*(1), 457–479. https://doi.org/10.1007/s00289-020-03120-8

Fadeyibi, A., Aina, S. J., Busari, R. A., Alabi, K. P., & Yisa, M. G. (2020). Optimization of Operation Parameters of a developed Dough Mixer. *LAUTECH Journal of Engineering and Technology*, *14*(2), 36–48.

Gai, Q. Y., Jiao, J., Wang, X., Luo, M., Gu, C. B., & Fu, Y. J. (2013). Microwave-assisted aqueous enzymatic extraction of oil from Isatis indigotica seeds and evaluation of its physicochemical properties, fatty acid compositions, and antioxidant activities. *Industrial Crops and Products*,

52, 587–594. https://doi.org/https://doi.org/10.1016/j.indcrop.2013.10.034

Gamage, P. K., Farid, A. S., & Karunanayake, L. (2009). Kinetics of degradation of PVC-containing novel neem oil as stabilizer. *Journal of Applied Polymer Science*, *112*(4), 2151–2165. https://doi.org/10.1002/app.29686

Ganorkar, R., Khan, S., & Chandramohan, K. (2023). Antidiabetic and Other Potential Features of Azadirachta indica A. Juss. (Neem). In *Antidiabetic Medicinal Plants and Herbal Treatments*. CRC Press.

Ghosh, P., Mitra, S., & Ray, S. (2022). Response surface optimization of vegetable oil extraction. *Chemical Engineering Research and Design*, *187*, 94–102. https://doi.org/https://doi.org/10.1016/j.cherd.2022.05.014

Ghoshal, G., & Sandal, S. (2024). Neem essential oil: Extraction, characterization, and encapsulation. *Food Chemistry Advances*, *4*, 100702. https://doi.org/10.1016/j.focha.2024.100702

Gomes, V. E. de S., Bócoli, P. F. J., Iamarino, J. G., Grimaldi, R., Ribeiro, A. P. B., & Marangoni Júnior, L. (2025). Neem Oil: A Comprehensive Analysis of Quality and Identity Parameters. *Lipidology*, *2*(2), 9. https://doi.org/10.3390/lipidology2020009

Gunstone, F. D. (2004). *The Chemistry of Oils and Fats: Sources, Composition, Properties, and Uses*. Blackwell Publishing Ltd.

Isman, M. B. (2015). A renaissance for Botanical Insecticides? *Pest Management Science*, *71*, 1587–1590. https://doi.org/https://doi.org/10.1002/ps.4088

Karaj, S., & Müller, J. (2011). Optimizing mechanical oil extraction of jatropha curcas L. seeds with respect to press capacity, oil recovery and energy efficiency. *Industrial Crops and Products*, *34*, 1010–1016. https://doi.org/https://doi.org/10.1016/j.indcrop.2011.03.009

Martinez, M. L., Bordon, M. G., Bodoira, R. M., Penci, M. C., Ribotta, P. D., & Maestri, D. M. (2017). Walnut and Almond oil screw-press extraction at industrial scale: Effects of process parameters on oil yield and quality. *Grasas Aceites*, *64*(4), e216. https://doi.org/http://dx.doi.org/10.3989/gya.0554171

Mohd, A. Z., Latif, M. A., & Ibrahim, M. S. (2022). Effects of screw press parameters on oxidation. *Journal of the American Oil Chemists' Society*, *99*, 57–68. https://doi.org/https://doi.org/10.1002/aocs.12578

Omowanle, J., Ayo, R. J., Habila, J., Ilekhaize, J., & Adegbe, E. A. (2018). PHYSICO-CHEMICAL AND GC-MS ANALYSIS OF SOME SELECTED PLANT SEED OILS; CASTOR, NEEM AND RUBBER SEED OILS. *FUW Trends in Science & Technology Journal*, *3*(2), 644–651.

Özturk, B., Koc, M., & Yildiz, G. (2020). Green extraction techniques for oil recovery: Challenges and prospects. *Food and Bioproducts Processing*, *122*, 234–245. https://doi.org/https://doi.org/10.1016/j.fbp.2020.04.004

Radočaj, O., Dimić, E., & Vujasinović. (2014). Optimization of the oil extraction process from pumpkin seed using response surface methodology. *Industrial Crops and Products*, *62*, 639–646.

Ramadan, M. F. (2023). *Bioactive Phtochemicals from Vegetable Oil and Oilseed Processing By-products*. Springer Nature. https://doi.org/10.1007/978-3-030-91381-6

Santos, K. D., Moraes, G. H., Noletto, A., & Sobral, P. (2024). Biopolymer-based coatings containing active ingrdients for cellulosic packaging: A review. *Cellulose*, *31*(13), 7841–7863. https://doi.org/https://doi.org/10.1007/s10570-024-06039-9

Sati, A., Nandiwdekar, O., Ratnaparkhi, A., Doke, R. B., Pinjari, D. V., Mali, S. N., & Pratap, A. P. (2025). Bio-Based Alkyd–Polyesteramide–Polyurethane Coatings from Castor, Neem, and Karanja Oils with Inherent Antimicrobial Properties for Enhanced Hygiene. *Coatings*, *15*(4), 370. https://doi.org/10.3390/coatings15040370

Savoire, R., Lanoisellé, J.-L., & Vorobiev, E. (2013). Mechanical Continuous Oil Expression from Oilseeds: A Review. *Food and Bioprocess Technology*, *6*(1), 1–16. https://doi.org/10.1007/s11947-012-0947-x

Schmutterer, H. (1990). Properties and potential of natural pesticides from the neem tree, Azadirachta indica. *Annual Review of Entomology*, *35*, 271–297.

Sharma, A., & Prasad, S. (2001). Extraction of oil from soybean using microwave pretreatment and mechanical pressing. *Journal of Food Engineering*, *50*(3), 273–277. https://doi.org/https://doi.org/10.1016/S0260-8774(00)00246-1

Taghvaei, M., Jafari, S. M., Assadpoor, E., Nowrouzieh, S., & Alishah, O. (2014). Optimization of microwave-assisted extraction of cottonseed oil and evaluation of its oxidative stability and physicochemical properties. *Food Chemistry*, *160*, 90–97. https://doi.org/https://doi.org/10.1016/j.foodchem.2014.03.064

Wang, X., Liu, Y., & Chen, H. (2020). Influence of microwave pre-treatment on oil yield and quality. *Food and Bioprocess Technology*, *13*(3), 457–468.

Yusof, M. S. M., Zainal, S., & Samsudin, R. (2017). Effect of screw speed and pre-treatment methods on palm kernel oil yield using screw press. *Chemical Engineering Transactions*, *56*, 1363–1368. https://doi.org/https://doi.org/10.3303/CET1756228

Zhang, J., Huo, X., Li, Y., & Strathmann, T. J. (2019). Catalytic Hydrothermal Decarboxylation and Cracking of Fatty Acids and Lipids over Ru/C. *ACS Sustainable Chemistry & Engineering*, *7*(17), 14400–14410. https://doi.org/10.1021/acssuschemeng.9b00215

Zhou, Y., Fan, W., Chu, F., & Pei, D. (2016). Improvement of the Flavor and Oxidative Stability of Walnut Oil by

Microwave Pretreatment. *Journal of the American Oil Chemists' Society*, *93*(12), 1563–1570. https://doi.org/https://doi.org/10.1007/s11746-016-2891-9

Zhuang, Y., Dong, J., He, X., Wang, J., Li, C., Dong, L., Zhang, Y., Zhou, X., Wang, H., Yi, Y., & Wang, S. (2022). Impact of Heating Temperature and Fatty Acid Type on the Formation of Lipid Oxidation Products During Thermal Processing. Frontiers in Nutrition, 9. https://doi.org/10.3389/fnut.2022.913297